THE JOURNAL OF PHYSICAL CHEMISTRY A

ARTICLE

pubs.acs.org/JPCA

Two-Dimensional Spectroscopy Can Distinguish between Decoherence and Dephasing of Zero-Quantum Coherences

Andrew F. Fidler,[†] Elad Harel,[†,§] Phillip D. Long,[‡] and Gregory S. Engel*[,†]

[†]The James Franck Institute and Department of Chemistry and [‡]Graduate Program in Biophysical Sciences, The University of Chicago, Chicago Illinois 60637, United States

ABSTRACT: Recent experiments on a variety of photosynthetic antenna systems have revealed that coherences among electronic states persist longer than previously anticipated. In an ensemble measurement, the observed dephasing of a coherent state can occur because of either disorder across the ensemble or decoherence from interactions with the bath. Distinguishing how much such disorder affects the experimentally observed dephasing rate is paramount for understanding the role that quantum coherence may play in energy transfer through these complexes. Here, we show that two-dimensional electronic spectra can distinguish between the limiting cases of homogeneous dephasing (decoherence) and inhomogeneous dephasing by examining how the quantum beat frequency changes within a cross peak. For the antenna complex LH2 isolated from *Rhodobacter sphaeroides*, we find that dephasing of the coherence between the B850 and B800 rings arises predominantly from inhomogeneity. In contrast, within the Fenna−Matthews−Olson (FMO) complex from *Chlorobium tepidum*, dephasing of the coherence between the first two excitons appears quite homogeneous. Thus, the observed dephasing rate sets an upper bound on decoherence for the LH2 complex while establishing both an upper and lower bound for the FMO complex.

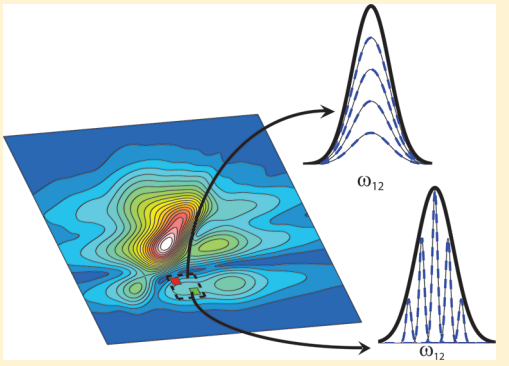

INTRODUCTION

Photosynthetic antenna complexes absorb radiation and guide the excitation energy to the reaction center where the energy results in charge separation that ultimately drives cellular metabolism. While the molecular structure of reaction centers is highly conserved across many different species, antenna complexes vary greatly, and the underlying microscopic mechanisms of how energy is guided through these systems are not currently fully understood.[1,2] Recent experiments[3−5] in a variety of antenna complexes have revealed that coherent mechanisms, in which the system is found in a superposition of excited electronic states, may contribute to the overall transfer efficiency of the complex,[6−8] and coherence has been shown to persist longer than the initial time scales for energy transfer even at physiological temperatures.[9−11]

Following excitation in a femtosecond experiment, the phase relationship between different members of the ensemble will be lost resulting in the observed decay of the coherent signal, which is referred to as dephasing. All ensemble experiments contain two contributions to the observed dephasing rate which arise from the same underlying mechanism but differ in time scales.[12] Static disorder across the ensemble results in a distribution of transition frequencies arising from differences in the microenvironments of the chromophores that do not vary appreciably over the time scale of the experiment. This distribution of frequencies causes the signal to dephase because of cancellation between signals from different elements of the ensemble. This mechanism is directly analogous to inhomogeneous broadening. In contrast, dynamic disorder that occurs faster than experimental time scales causes every element of the ensemble to decohere in analogy to homogeneous broadening. The key distinction is that this decoherence arises from interactions of the system with the environment occurring on time scales faster than or commensurate with the experimental time scale, causing the transition frequency of all members of the ensemble to appear identical. This form of decoherence provides a true measure of the lifetime of the coherence in question. Inhomogeneous dephasing implies that, although the ensemble dephases rapidly, individual elements of the ensemble, if measured separately, might decohere much more slowly.[13] Most systems in the condensed phase will exist in an intermediate regime where multiple degrees of freedom, each with their own distinct time scales, contribute to the observed dephasing rate.[14] However, if there is a separation of time scales relative to the experimental time scale, one can separate the faster components into a homogeneous contribution and the slower components into an inhomogeneous contribution. Proteins in solution comprise one of these examples where ultrafast measurements of correlation functions have shown fast subpicosecond components, picosecond relaxation, and longer-lived components that appear to not decay on the time scale of several picoseconds or longer.[15] Thus, for coherences that last at most a few picoseconds, there is a clear separation of time scales and we can treat the much longer-lived components as a static distribution of transition frequencies.[12]

Received: September 12, 2011
Revised: November 2, 2011

Distinguishing whether the coherence dephases predominantly in the inhomogeneous limit (dephasing) or the homogeneous limit (decoherence) will reveal if the measured coherence lifetime represents either a lower bound or both an upper and lower bound for the relevant time scale of the coherent dynamics. This distinction will aid in the understanding of the relative contribution of coherent mechanisms in photosynthesis.

Various spectroscopic methods are capable of directly quantifying inhomogeneity for excited states in the single-quantum coherence manifold, i.e., the transition between the ground and excited electronic states. Hole-burning spectroscopy and the closely related fluorescence line narrowing spectroscopy have been used at low temperatures to measure the inhomogeneous line widths for a variety of samples.[16,17] These techniques rely on the approximation of slow spectral diffusion (which is not applicable at room temperature) so that inhomogeneous line widths dominate broadening in the condensed phase. Photon echo peak shift experiments have also been shown to separate homogeneous and inhomogeneous spectral diffusion by rephasing the static inhomogeneity.[14,18] These experiments allow direct measurement of the correlation function and enable determination of the relevant time scales for solvent reorganization in the condensed phase. However, these experiments are not sensitive to the phase of the signal, nor do they provide spectral resolution within the pulse envelope. Thus, these measurements usually preclude isolating signals that arise from coherent superpositions in spectrally congested systems.

Here, we use a closely related method, two-dimensional spectroscopy,[19,20] which correlates absorption events with emission events as a function of a waiting time. Briefly, three noncollinear femtosecond laser pulses are incident on the sample, generating a degenerate four-wave mixing signal in a phase-matched direction. During the first time delay the system is prepared into a superposition between the ground and resonant electronic excited states, which evolves phase as a function of coherence time, τ. The next pulse promotes the coherence to either a population or zero-quantum coherence, i.e., a superposition of excited states, which is then allowed to evolve for a waiting time, T. The final pulse stimulates the emission of the third-order response and the time delay between the final pulse and emitted signal is detected a time, t, later. The timings between beams are then parametrically scanned and a two-dimensional Fourier transform is performed over τ and t to generate a two-dimensional correlation spectrum. Coherent signatures between electronic states can be observed in this spectrum by examining how the cross peak amplitude oscillates with waiting time. If coherence is maintained, the cross peak amplitude will beat at the frequency difference between the excited states damped by the dephasing rate in addition to decay or growth due to population dynamics.

In this paper we investigate the observed dephasing and its dependence on inhomogeneity in the sample. We will show that current two-dimensional (2D) spectroscopy experiments can in fact distinguish whether the observed dephasing rate predominantly arises from inhomogeneity in the sample or is limited by the lifetime of the state. The ability to distinguish between these two cases arises from the fact that the beating signal can differ throughout the cross peak. We will first present a model for a coupled two-chromophore system, more rigorously define homogeneous and inhomogeneous broadening, and then present a derivation of how these processes are manifested in the experiment. Next we will present experimental work on two different light-harvesting complexes that demonstrate the character of the limiting cases of our model. We will conclude with a discussion of the results.

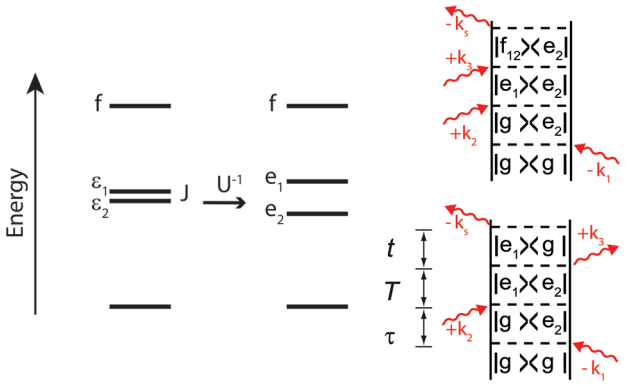

Figure 1. Schematic of a coupled two-chromophore system in the site basis (left) and exciton basis (right) which are related through a unitary transformation U^{-1}. The two Feynman diagrams that contribute to coherent beating below the diagonal in a rephasing experiment are shown.

MODEL

We utilize a coupled two-chromophore system developed by Yang and Fleming to explore the effects of inhomogeneity on the nonlinear response.[21] Here we present the main features of the model. We begin by writing the zero-order Frenkel exciton Hamiltonian in second quantized notation:

$$H_0 = e_1 a_1^\dagger a_1 + e_2 a_2^\dagger a_2 + J(a_1^\dagger a_2 + a_2^\dagger a_1) + H_{\mathrm{ph}}$$

Here $a_i^\dagger$ (a_i) is the creation (annihilation) of an exciton on site i with energy e_i. J denotes the coupling between the two chromophores and is assumed to be purely real, and H_{ph} is the Hamiltonian for the phonon bath. To a good approximation even in multichromophoric systems, the beating feature between two excitonic states in the rephasing spectra either above or below the diagonal results from only two pathways involving a single biexciton state and not every possible biexciton state as shown in Figure 1. The two chromophores are then coupled to a bath of phonons, which we will assume is diagonal in the site basis, i.e., that fluctuations in the coupling constant are small in comparison with fluctuations in the site energies.

$$H_{e-ph} = q_1(Q) a_1^\dagger a_1 + q_2(Q) a_2^\dagger a_2$$

Here $q_i(Q)$ is the bath operator which describes the fluctuations in the site energy of chromophore i with the property $\langle q_i(Q)\rangle = 0$, meaning stationary contributions of the bath are incorporated into the zero-order Hamiltonian. We will further assume that the fluctuations are Gaussian in nature and that the site energy fluctuations are statistically independent of each other, so the frequency−frequency correlation function for each chromophore fully defines the system bath interaction. The frequency−frequency correlation function of chromophore i is defined as

$$C_i(t) = \frac{1}{\hbar^2}\langle q_i(t)\, q_i(0)\rangle$$

Here the time evolution is determined with respect to the phonon bath Hamiltonian. We then diagonalize the Hamiltonian matrix into the exciton basis via a unitary transformation, where the exciton correlation functions, transition energies, and transition dipoles become a linear combination of the site basis parameters.

dx.doi.org/10.1021/jp2088109 |J. Phys. Chem. A XXXX, XXX, 000–000

We will assume that inhomogeneity in the sample will alter the optical frequency of the transition, while the underlying dynamic fluctuations will remain conserved across the ensemble; i.e., the spectral density is the same for all members of the ensemble.[12] Hence, we can partition the response function into (1) a homogeneous contribution, where contributions to the correlation function decay on time scales commensurate with the experiment, and (2) the inhomogeneous contribution including those fluctuations which decay with time scales significantly longer than the experimental time scale and therefore act to shift the transition frequencies.[12] At long enough time scales the system will sample all possible states and the distinction is meaningless, but at short time scales where coherence is maintained, this separation of time scales is rigorous. Physically, the slower degrees of freedom represent different protein conformations or solvent configurations which persist for at least nano- to microseconds. Other types of inhomogeneity theoretically could exist, where different members of the ensemble have different spectral densities, and our analysis cannot decouple this information. We note that fluorescence line narrowing experiments have not found such an environment for photosynthetic antenna complexes; that is, excitation of different regions of the inhomogeneous band yielded the same spectral density.[22] In this regime, we can write the linear response function as the following:

$$J_{\text{ensemble}}(t) = \int \mathrm{d}\Gamma\, W(\Gamma)\, J(t,\Gamma) = J_{\text{H}}(t)\, \chi(t)$$

Here Γ is a parameter representing the slower degrees of freedom with normalized distribution function $W(\Gamma)$, $J_{\text{H}}(t) = \langle V_{\text{ge}}(t)\, V_{\text{eg}}\rho_{\text{g}}\rangle$ is the homogeneous contribution to the linear response, and $\chi(t) = \int \mathrm{d}\Gamma\ W(\Gamma)\ \exp(-\mathrm{i}(\omega_{\text{eg}}(\Gamma) - \langle\omega_{\text{eg}}\rangle)t)$ is the inhomogeneous contribution. The Fourier transform of the linear response is the absorption spectrum and will yield a convolution of homogeneous and inhomogeneous line shapes, with separate relative line widths which will be referred to as homogeneous and inhomogeneous line widths.

$$A(\omega) = \int_{-\infty}^{\infty} \mathrm{d}\omega'\, \sigma(\omega - \omega')\, W(\omega')$$

where $A(\omega)$ is the linear absorbance spectrum, $\sigma(W)$ is the Fourier transform of $J_{\text{H}}(t)$, and similarly $W(\omega)$ is the Fourier transform of $\chi(t)$. Similarly, we can partition the third-order response into homogeneous and inhomogeneous contributions:[12]

$$\begin{aligned} R(t,T,\tau)_{\text{ensemble}} &= \int W(\Gamma)\, R(t,T,\tau,\Gamma) \\ &= R_{\text{H}}(t,T,\tau)\, \chi(t-\tau) \end{aligned}$$

The signature of electronic coherence among excitons in two-dimensional spectroscopy is the beating observed in the cross peaks in the rephasing portion of the response. For each pair of excitons, approximately one pair of Liouville space pathways, i.e., Feynman diagrams, contributes to the observed beating in a cross peak above or below the diagonal as shown in Figure 1. Utilizing the cumulant expansion within the secular approximation, these two response functions can be calculated explicitly.[23] Other energy transfer pathways will also contribute to the observed response, giving rise to additional contributions that typically increase or decrease exponentially with population time and can be numerically removed in postprocessing of the data.

For the cumulant expansion expression of the response function, the Fourier transform over the first two time delays cannot be performed analytically. However, if we further make the stationary phase approximation, then the Fourier transform can be performed analytically, and we can explicitly calculate the functional form of the beating signal between states a and b. This approach assumes that we can take a Taylor expansion of the correlation functions with respect to the first two time arguments, because the coherence between the ground and excited states decays quickly.[18,23] The beating signal is then given by

$$\begin{aligned} S_{\text{beat}}(\omega_\tau, T, \omega_\tau) &= (\langle \mu_{gb}\mu_{bg}\mu_{ga}\mu_{ag}\rangle - \langle \mu_{gb}\mu_{bf}\mu_{fa}\mu_{ag}\rangle) \\ &\times \int \mathrm{d}\Gamma\ W(\Gamma)\ \exp(\mathrm{i}(\omega_a(\Gamma) - \omega_b(\Gamma))T + f(T))G\{\omega_\tau - \omega_b(\Gamma), \delta^2(T)\} \\ &\times G\left\{\omega_\tau - \omega_a(\Gamma) + Q(T) + \frac{H(T)(\omega_\tau - \omega_b(\Gamma))}{\delta^2(T)}, \Delta^2(T) - \frac{H^2(T)}{\delta^2(T)}\right\} \end{aligned}$$

where the broken brackets $\langle\cdots\rangle$ represent an orientional average over the dipoles, $G\{x,y\} = (2\pi/y)^{1/2}\mathrm{e}^{-x^2/2y}$ is a normalized Gaussian, and $f(T), H(T), Q(T), \Delta(T)$, and $\delta(T)$ are auxiliary functions given in the Appendix. The form for the beating below the diagonal will be of identical form as above the diagonal and can be obtained by simply switching indices a and b. Here we see that for each choice of ω_t and ω_τ there will be many contributions from different members of the inhomogeneous band arising from the finite peak width for each member of the ensemble. Further, the beat frequency at each point is dependent on the sum of the contributing beat frequencies, thus changing the observed beat frequency as well as its lifetime, meaning the inhomogeneity acts to artificially shorten the observed dephasing rate. The effect of the inhomogeneity depends critically on the inhomogeneous distribution, $W(\Gamma)$. If we assume that different members of the ensemble in the inhomogeneous band conserve the energy gap between the exciton levels, then the beat frequency will be identical for all members of the ensemble, and further because the initial phase is set by the applied laser pulses, they will all beat in phase and hence the observed beating will not be shortened due to the energetic inhomogeneity. Thus, even a sample with significant inhomogeneity does not necessitate that the observed zero-quantum coherence be artificially shortened due to the ensemble measurement. That is, the correlation in the static disorder among excitonic energies will determine whether the zero-quantum coherence dephases with homogeneous or inhomogeneous character.

Intuitively, this analysis can be understood by considering the limiting cases of the model. For homogeneous dephasing processes, we expect that beating within a cross peak should beat with a single frequency at all points within the cross peak because we observe only the ensemble average of the beating frequency: $S(T) = \langle\exp(i(\omega_\tau - \omega_t)T\rangle$. In this homogeneous limit, fast dynamics cause a complete loss of correlation between the observed transition frequencies during the first and third time periods causing the observed difference frequency between them to remain constant. For an inhomogeneously broadened system we must explicitly consider the slower degrees of freedom in the system that give rise to a static distribution of transition frequencies during the experiment. In this case, the signal is a function of not only time, but also of the observed single-quantum transition frequencies: $S(\omega_\tau,T,\omega_t) = \langle\exp(\mathrm{i}(\omega_\tau - \omega_t)T\rangle$. In essence, different members of the ensemble show different beat frequencies, and the two-dimensional photon echo spectroscopy can resolve these subensembles based on their transition energies. For inhomogeneous dephasing processes, the frequency of the beating should follow the energy difference between the ω_t and ω_τ axes.

dx.doi.org/10.1021/jp2088109 |J. Phys. Chem. A XXXX, XXX, 000–000

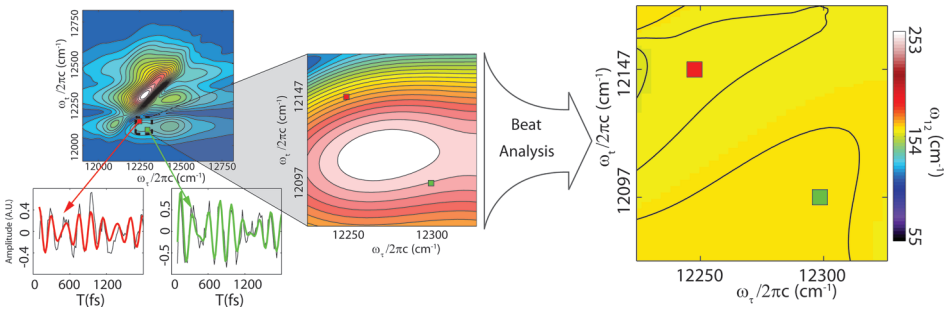

Figure 2. Representative two-dimensional spectra of FMO from *C. tepidum* taken at 77 K and waiting time of 1870 fs. The beating signal in a 100 cm^{-1} × 100 cm^{-1} region highlighted around the exciton 1−2 cross peak is analyzed to determine the 1−2 beat frequency throughout the cross peak region. The exciton 1−2 beat frequency throughout the cross peak is shown with contour lines drawn for every 2 cm^{-1} interval, and the color axis indicates the range expected for a purely inhomogeneous dephasing process. Beating signals are extracted from two representative points within the region and show little change in the beat frequency for FMO.

In general, broadening will occur via both mechanisms. By examining the quantum beating at all points across the off-diagonal feature in a 2D electronic rephasing spectrum, we can distinguish between the two processes. For a purely inhomogeneously broadened peak we expect to measure a change in the beat frequency commensurate with the size of the feature, while a purely homogeneously broadened peak will show no dependence of the beat frequency on the location in the cross peak.

To further support this result, we have numerically calculated the response function in the intermediate regime, where multiple contributions to the correlation function with distinct time scales. We assume delta function pulses and model the inhomogeneous distribution as Gaussian with 220 cm^{-1} full width at half-maximum (fwhm). The spectral density of the solvent was modeled as Ohmic, $C(\omega) = \lambda(\omega/\omega_c)\exp[-(\omega/\omega_c)]$, with a cutoff frequency of 60 cm^{-1} and a coupling strength of 35 cm^{-1}. These values and model are typical for photosynthetic antenna complexes.[23] The correlation function can then be calculated from the spectral density using standard methods.[12] The temperature was set to 77 K, the coupling constant J was 220 cm^{-1}, and the energy difference between the sites was 680 cm^{-1}. We further assume the inhomogeneous distribution causes the site energies to change, while the coupling constant remains fixed. We model the inhomogeneous distribution in two ways. First, we allow the two site energies to change independently of each other. We refer to this model as uncorrelated inhomogeneity. In the second case the energy gap between the two sites is conserved; hence the energy gap between the excitonic states remains constant as does the observed beat frequency. We will refer to this model as correlated inhomogeneity. This model will give rise to homogeneous dephasing because the gaps between excitons are homogeneous. We will discuss the results of the model calculations in the Discussion section.

EXPERIMENTS

The Fenna−Matthews−Olson (FMO) complex from *Chlorobium tepidum* was isolated as previously described.[24] A concentrated sample was mixed with 800 mM Tris·HCl buffer and dissolved in 35:65 vol/vol glycerol water solution with 0.1% lauryldimethylamine oxide (LDAO) detergent resulting in an optical density of 0.32 at 809 nm in a 200-μm fused silica cell. A cryostat was used to cool the sample to 77 K, and 2D spectra were collected using a diffractive optics based spectrometer.[25,26]

The output from a 5 kHz regenerative amplifier was split by a beam splitter to create a pair of pulses with a relative delay controlled by a retro reflector attached to a computer controlled translation stage. The two pulse pairs were focused onto a diffractive optic, and the +1 and −1 order diffraction spots from each beam were focused onto the sample in boxcar geometry with a spot size of ∼70 μm^2. The pulse energy at the sample was 1.6 nJ/pulse with a pulse width of 38 fs fwhm determined from second harmonic autocorrelation. The timing of beams 1 and 2 was controlled by a pair of matched fused silica wedges mounted to translation stages, and the local oscillator beam was attenuated by a factor of 1000. For each spectrum the coherence time was sampled from −500 to 500 fs with a step size of 4 fs and the waiting time was sampled in steps of 20 fs to a maximum waiting time of 1800 fs. The signal was then spectrally resolved onto a charge coupled device. Scatter subtraction and data analysis have been described previously.[25] The resulting resolution was 3.7 cm^{-1} in the ω_τ domain and 1.3 cm^{-1} in the ω_t domain.

Light-harvesting complex LH2 was isolated from *Rhodobacter sphaeroides* and dissolved in a 20 mM Tris·HCl solution with 1.3% LDAO resulting in an optical density of 0.2−0.3 at 800 nm in a 200-μm fused silica flow cell. The output from a regenerative amplifier was focused into argon to produce a spectrally broadened pulse spanning from ∼750 to 850 nm that was compressed to ∼25 fs with chirped mirrors. A GRAPE spectrometer[27−29] was then used to acquire rephasing two-dimensional spectra. Briefly, the spectrally broadened pulse was split by a 50/50 beam splitter and the relative timings between the pulse pair were controlled with a retro reflector on a computer controlled translation stage. The two pulses were then split to four via the front and back Fresnel reflections off an uncoated, wedged, fused silica optic and focused onto the sample with a cylindrical lens in a distorted boxcar geometry. This distortion created a time gradient between pulses 1 and 2 across the sample which was then imaged into a spectrometer and measured with a charge coupled device. The waiting time was sampled every 10 fs to a maximum of 2 ps, and the coherence time gradient was set to −100 to 300 fs across the sample with 0.5 fs per pixel on the camera. Scatter subtraction and data analysis have been described previously.[27] The resulting resolution was 32 cm^{-1} in the ω_τ domain and 16.5 cm^{-1} in the ω_t domain after binning of the signal to improve the signal-to-noise ratio.

The absolute value of the rephasing spectrum for both LH2 and FMO was analyzed for beating off the diagonal. While it

dx.doi.org/10.1021/jp2088109 |J. Phys. Chem. A XXXX, XXX, 000–000

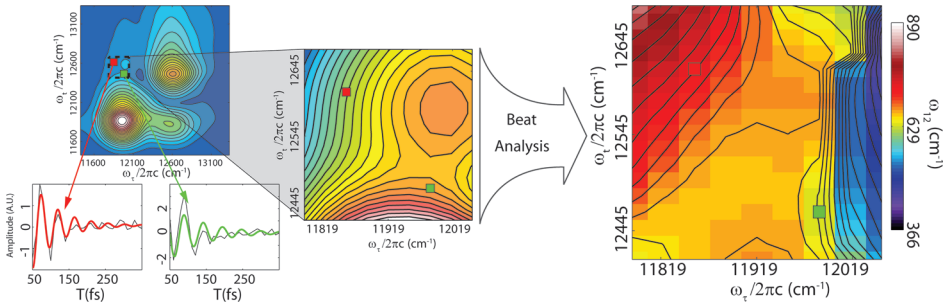

Figure 3. Representative two-dimensional spectra of LH2 from *R. sphaeroides* taken at 294 K and waiting time of 390 fs is shown (left). The beating signal in a 260 cm^{-1} × 260 cm^{-1} region highlighted near the upper B800−B850 cross peak was analyzed to determine the beat frequency throughout the cross peak. The B800−B850 beat frequency throughout the cross peak is shown with contour lines drawn for every 15 cm^{-1} interval, and the color axis indicates the range expected for a purely inhomogeneous dephasing process. Beating signals are extracted from two representative points within the region and show a change in beat frequency for LH2.

would be ideal to fit the beating in only the real portion, the LH2 data were not phased because the GRAPE spectrometer only measures the rephasing portion of the third-order signal, and phasing to pump−probe signal requires the acquisition of nonrephasing signal as well. Fitting to the absolute value of the signal will not affect the beat frequency and thus will not affect the results of this paper.

DISCUSSION

Shown in Figure 2 are data taken from the FMO antenna complex of *C. tepidum* green sulfur bacteria at 77 K. A 100 cm^{-1} × 100 cm^{-1} region centered around the exciton 1−2 cross peak was then investigated. Slow population dynamics and dispersive contributions were first removed by fitting to two exponential decays and subtracting the fit from the signal. The residual was then fit to two exponentially decaying sinusoids corresponding to the 1−2 and 1−3 coherences, and this procedure was repeated for every point within the selected region. We chose to fit to two sinusoids because a Fourier transform of the waiting time shows two distinct peaks at high frequencies. Directly analyzing the Fourier transform does not show either peak to shift when comparing different locations in the cross peak. Due to the finite width of the exciton 1−3 cross peak, both beating features are observed in the region. The initial guess to the nonlinear least-squares fitting algorithm assigns the beat frequencies from the Fourier transform, but all parameters float to produce the best fit. Two representative fits are shown which reveal good agreement with the data. The beat frequencies are constrained to remain within ±270 cm^{-1} of the initial value to ensure the fitting algorithm does not diverge. A two-dimensional beating map can then be created, which reveals how the beating frequency changes throughout the selected region of the cross peak. The color map is set to run from the minimum to the maximum expected beat frequency corresponding to the limiting case of pure inhomogeneous dephasing, i.e., the difference between the frequency axes at the top left corner to the difference at the bottom right corner. This coloration facilitates comparison between this experiment and those on other complexes and automatically controls for the different sizes of the regions of interest. Examining the 1−2 beat frequency fit reveals that over the 100 cm^{-1} square the beat frequency changes by only ∼9 cm^{-1}, which is ∼5% of the theoretical limit for inhomogeneous broadening; i.e., for a 100 cm^{-1} region we would expect the beat frequency to change by 200 cm^{-1}. We therefore conclude that at, 77 K, the zero-quantum coherence between excitons 1 and 2 can be characterized as predominantly homogeneously broadened in FMO. That is, the energy gaps between excitons are quite homogeneous.

A different pattern is evident in 2D spectra from the LH2 antenna complex from purple bacteria at ambient temperature, shown in Figure 3, where we have recently observed coherence maintained between the B800 and B850 rings.[28] We have assigned this feature to transfer from the lower lying states in the B800 ring to the $k = \pm 1$ state of the B850 ring, because the other states that lie in the B850 band have significantly weaker dipoles. We do not see evidence for high lying k states due to experimental noise.[28] Supporting this assignment, we only observe one frequency component at any particular point in the cross peak. The coherent beating signal is extracted from a 260 cm^{-1} × 260 cm^{-1} region centered on a cross peak above the diagonal. While beating should be observed both above and below the diagonal in equal intensity according to our model, we do not see significant beating below the diagonal. This may be because complexity of population relaxation on the lower cross peak forbids a clean separation of the beating signature in LH2. Regardless, the pattern in the beating map of the cross peak should be identical above and below the diagonal. Slow population dynamics and dispersive components were similarly removed by fitting to two exponential decay functions. The residual was then fit to a single exponentially decaying sinusoid, corresponding to the observation of a single peak in the Fourier transform of the waiting time. Two representative fits are shown. The beat frequency was constrained to remain within ±2000 cm^{-1} of the initial guess to ensure convergence. In LH2, we observe a strong dependence of the beat frequency on the location within the cross peak with the beat frequency changing by ∼375 cm^{-1}, which is ∼71% of the theoretical limit for inhomogeneous broadening; i.e., for a 260 cm^{-1} region we would expect the beat frequency to change by 520 cm^{-1}. We conclude that inhomogeneity contributes significantly to the observed dephasing. This inhomogeneous broadening implies that, for an individual member of the ensemble, coherence persists longer than can be experimentally observed. In essence, the coherence appears artificially shortened due to inhomogeneity in the sample. Put differently, dephasing is fast, but decoherence is slow. Therefore, although it appears that quantum coherence disappears in 350 fs, coherence may well affect dynamics at longer time scales. Naively, we can speculate that if dephasing occurs in 350 fs and is 71% inhomogeneously broadened, then the decoherence time should be on the order of 1 ps—long enough to affect energy transfer in LH2 (800 fs).

dx.doi.org/10.1021/jp2088109 |*J. Phys. Chem. A* XXXX, XXX, 000–000

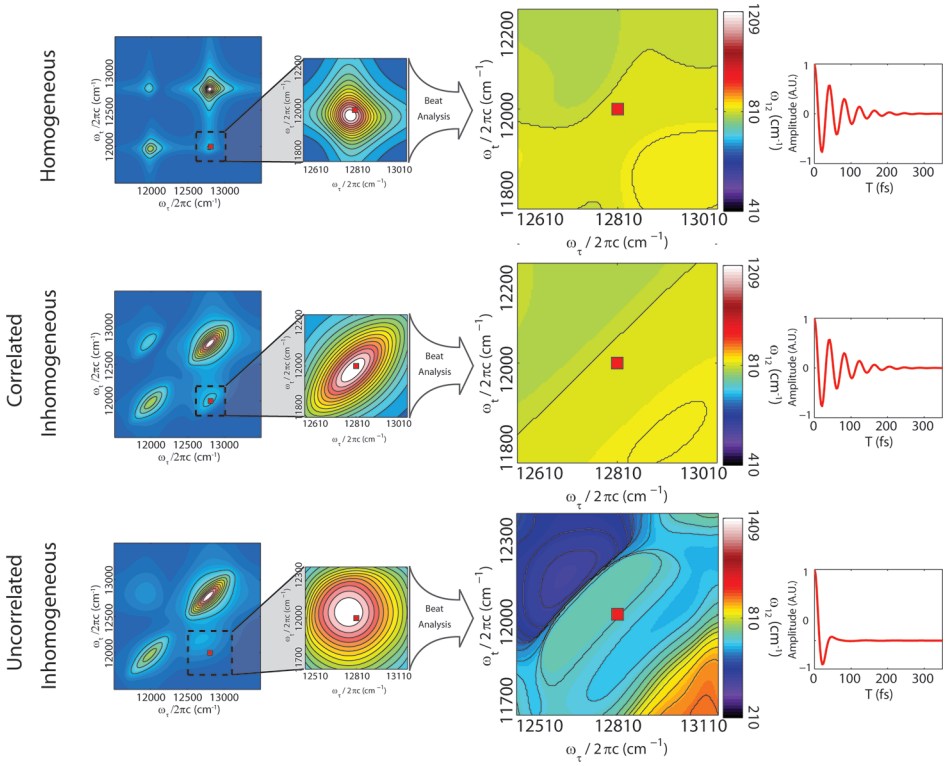

Figure 4. Model calculations of the dephasing of electronic coherence in the intermediate regime. The two-dimensional spectrum at a waiting time of zero is shown, and the lower cross peak was analyzed in the same manner as the experiments. The first row shows the case of no static inhomogeneity in the system. A 400 $cm^{-1} \times 400\ cm^{-1}$ region was selected around the cross peak, and the beat frequency was then found throughout the region. The beat frequency does change significantly with respect to the size of the feature. Contour lines are drawn every 20 cm^{-1}, and the color map is determined by the expected change in beat frequency for the inhomogeneous limit. The next row shows correlated inhomogeneity and the same size region was again selected. This results in a qualitatively identical beat map and no change in the dephasing rate. The final row shows uncorrelated inhomogeneity. The region around the cross peak was extended to a 600 $cm^{-1} \times 600\ cm^{-1}$ region in order to fully encompass the cross peak. This reveals a significant change in the beat frequency with location in the cross peak relative to the size of the feature. The dephasing rate is also significantly suppressed due to the inhomogeneity in the system. Contours for the beat map were drawn for every 30 cm^{-1}, and the color map is determined by the expected change in beat frequency for the inhomogeneous limit.

The main features of the experiments can be reproduced by our model. Shown in Figure 4 are the results of the model calculation. We select a 400 $cm^{-1} \times 400\ cm^{-1}$ region around the cross peak signal and find the beat frequency for each pixel within the region by locating the maximum of the Fourier transform. For the case in which there is no static inhomogeneity in the system, the observed beat frequency does not change significantly throughout the cross peak region as expected. The small, finite change in beat frequency results from the correlation function decaying on time scales similar to the beating. Next, if we add inhomogeneity into the system in a correlated fashion, the beat frequency again does not change and the observed dephasing rate is identical to the homogeneous case. Finally, when inhomogeneity is added in an uncorrelated fashion, the beat frequency changes throughout the cross peak, and the dephasing rate is larger than in the homogeneous case. Note that the region of interest has been increased for the uncorrelated inhomogeneity case in order to fully encompass the cross peak. We note that the addition of correlated fluctuations and allowing for off-diagonal fluctuations changes the dephasing rate but not the beating map.

The amount of inhomogeneous broadening in the zero-quantum manifold is a measure of the static degree of correlation between the excitonic transitions, as shown in Figure 5. The FMO complex, in which we observe little change in the beat frequency, requires that while different members of the ensemble have different mean energy levels, the gap between them remains roughly constant across the ensemble. Thus, the states are highly correlated across the inhomogeneous ensemble. For LH2, the static disorder between the B800 and B850 states appears uncorrelated, causing the energy difference between these states to change appreciably for different members of the ensemble. While these two data sets were taken at different temperatures, we believe that the observed features are not a result of temperature differences. While we do have room temperature data for FMO protein, the beating only goes though ~1.5 cycles of beating before dephasing, making it difficult to measure if the beat frequency does change throughout the cross peak.[11]

We attribute this difference between FMO and LH2 to be largely due to the remarkably different molecular structures. In FMO, the average chromophore separation within a monomer is ~12 Å,[29] while in LH2 the closest separation between the B850 and B800 chromophores is ~18 Å and can be as far as 60 Å.[30] Further, the protein environments for the B850 and B800 chromophores are quite different, varying in their degree of exposure to the solvent and differing nearby residues, while for FMO the chromophores are held within a similar environment, all being pinned between two large beta sheets. In this way, the protein

dx.doi.org/10.1021/jp2088109 |J. Phys. Chem. A XXXX, XXX, 000–000

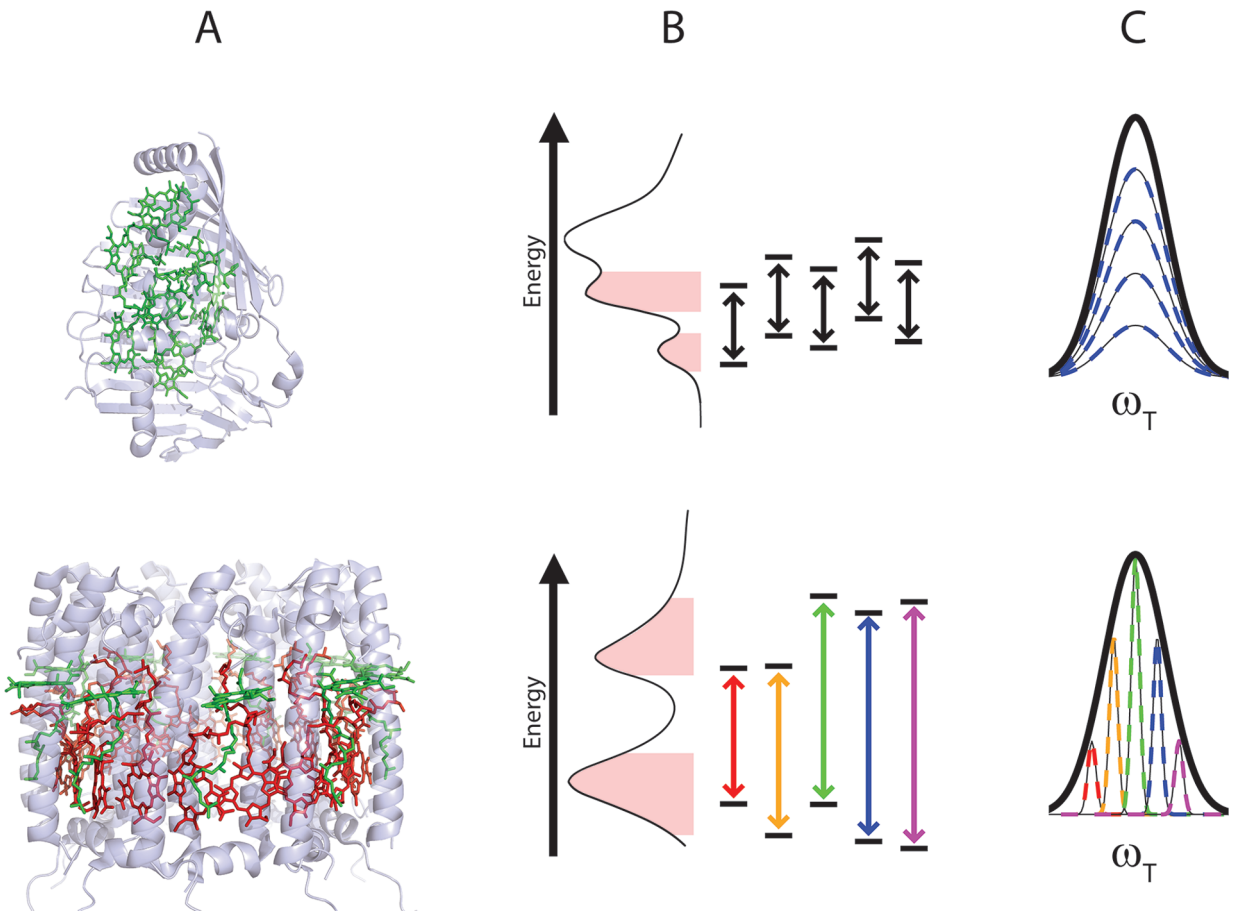

Figure 5. (A) Crystal structure of FMO (upper) and LH2 (lower) to scale. (B) For FMO, different members of the ensemble differ in exciton energy levels, but the relative gap remains constant, while for LH2 the energy gap does not remain constant. Also shown is the linear absorbance spectrum where the coherence between the highlighted regions is investigated. (C) The correlation of the energy gap across the ensemble leads to homogeneous broadening for FMO and inhomogeneous broadening for LH2.

environment in FMO correlates the static excitonic energy levels, causing the energy difference to remain constant. In this respect it is rather surprising that the measured lifetime against dephasing of 80 fs for LH2 is rather close to the 133 fs dephasing rate of FMO at room temperature.[11] Because the B850 and B800 states are weakly coupled and therefore share little character in the site basis, it would seem that correlated site fluctuations would be needed to maintain coherence for the observed time.[5] Correlation of inhomogeneity has also been observed in two-dimensional infrared experiments, where the cross peaks were separated enough to observe this effect through the line shape of the cross peak.[31]

The observed dephasing of zero-quantum coherences in two-dimensional spectroscopy sets a lower bound for the time scales of coherent quantum dynamics, and analyzing the structure of the cross peak can determine if this lower bound also represents an upper bound for the coherence lifetime. While we can distinguish between the limiting cases, our spectroscopy currently cannot directly measure the homogeneous and inhomogeneous line widths. It should be possible to rephase the zero-quantum coherence at short time delays, for example in a higher-order MUPPETS-like experiment,[32] in much the same way that two-dimensional spectroscopy rephases the one-quantum coherences. This approach would permit complete characterization of the relative contributions to the dephasing of the zero-quantum coherence.

APPENDIX

The auxiliary functions for the beating signal are given by

$$f(T) = -g_1^*(T)\cos^4\theta - g_2^*(T)\sin^4\theta - g_1(T)\sin^4\theta - g_2(T)\cos^4\theta + \kappa^2\,\mathrm{Re}[g_1(T) + g_2(T)]$$

$$\delta^2(T) = \kappa^2\{C_1(0) + C_2(0)\} + \cos(2\theta)\,\mathrm{Re}[C_1(T)\cos^2\theta - C_2(T)\sin^2\theta]$$

$$\Delta^2(T) = \kappa^2\{C_1(0) + C_2(0)\} - \cos(2\theta)\,\mathrm{Re}[C_1(T)\sin^2\theta - C_2(T)\cos^2\theta]$$

$$H(T) = \kappa^2\,\mathrm{Re}[C_1(T) + C_2(T)]$$

$$S(T) = -\sigma_1(T)\sin^2\theta - \sigma_2(T)\cos^2\theta$$

Here the mixing angle $\theta = (1/2)\arctan(2J/(e_1 - e_2))$, delocalization constant $\kappa = \cos\theta\sin\theta$, line shape function $g_i(t) = \int_0^t \int_0^\tau C_i(\tau')\,\mathrm{d}\tau'\,\mathrm{d}(\tau)$, and Stokes shifting function $\sigma_i(t) = \mathrm{Im}[\int_0^t C_i(\tau)\,\mathrm{d}\tau]$.

dx.doi.org/10.1021/jp2088109 |J. Phys. Chem. A XXXX, XXX, 000–000

The two response functions for the coherent beating signal without the stationary phase approximation are

$$\langle \mu_{ge_2}\mu_{e_2g}\mu_{ge_1}\mu_{e_1g}\rangle \exp[i\omega_{e_2g}\tau + i(\omega_{e_2g} - \omega_{e_1g})T - \omega_{e_1g}t] \exp[-g^*_{e_2e_2}(\tau + T) + g^*_{e_2e_1}(\tau + T + t) - g^*_{e_2e_1}(\tau) - g^*_{e_2e_1}(t) + g_{e_2e_1}(T) - g_{e_1e_1}(T + t)]$$

$$-\langle \mu_{ge_2}\mu_{e_2f}\mu_{fe_1}\mu_{e_1g}\rangle \exp[i\omega_{e_2g}\tau + i(\omega_{e_2g} - \omega_{e_1g})T - \omega_{e_1g}t] \exp[-g^*_{e_2e_2}(\tau + T + t) + g^*_{e_2f}(\tau + T + t) - g^*_{e_2f}(\tau + T) + g^*_{e_2e_1}(\tau + T) - g^*_{e_2e_1}(\tau) + g_{e_2f}(t) - g_{e_2e_1}(t) + g_{e_2e_1}(T + t) - g_{ff}(t) + g_{e_1f}(t) - g_{e_1f}(\tau + T + t) + g_{e_1f}(T) - g_{e_1e_1}(T)]$$

Here the excitonic line shape functions and dipoles are a linear combination of the site basis line shape functions

$$g_{e_1e_1}(t) = g_1(t)\cos^4\theta + g_2(t)\sin^4\theta$$

$$g_{e_2e_2}(t) = g_1(t)\sin^4\theta + g_2(t)\cos^4\theta$$

$$g_{ff}(t) = g_1(t) + g_2(t)$$

$$g_{e_1e_2}(t) = \kappa^2\{g_1(t) + g_2(t)\}$$

$$g_{e_1f}(t) = g_1(t)\cos^2\theta + g_2(t)\sin^2\theta$$

$$g_{e_2f}(t) = g_1(t)\sin^2\theta + g_2(t)\cos^2\theta$$

$$\mu_{e_1g} = d_1\cos\theta + d_2\sin\theta$$

$$\mu_{e_2g} = -d_1\sin\theta + d_2\cos\theta$$

$$\mu_{e_1f} = d_1\sin\theta + d_2\cos\theta$$

$$\mu_{e_1g} = d_1\cos\theta - d_2\sin\theta$$

AUTHOR INFORMATION

Corresponding Author

*E-mail: gsengel@uchicago.edu.

Present Addresses

[§]Department of Chemistry, Northwestern University, Evanston IL, 60208, United States.

ACKNOWLEDGMENT

The authors would like to thank DARPA (Grants N66001-10-1-4060 and N66001-10-1-4022) and the Searle Foundation for support. A.F.F. and P.D.L. would like to acknowledge support from the DOE SCGF program. E.H. would like to acknowledge support from National Science Foundation Grant DMR-0844115 and the Institute for Complex Adaptive Matter Branches Cost-Sharing Fund.

REFERENCES

(1) Blankenship, R. E. *Molecular Mechanisms of Photosynthesis*; Blackwell Science: Oxford, 2002.
(2) van Amerongen, H.; Valkunas, L.; van Grondelle, R. Exciton Dynamics. In *Photosynthetic Excitons*; World Scientific: Singapore, 2000; Chapter 8.
(3) Calhoun, T. R.; Ginsberg, N. S.; Schlau-Cohen, G. S.; Cheng, Y. C.; Ballottari, M.; Bassi, R.; Fleming, G. R. *J. Phys. Chem. B* **2009**, *113*, 16291.
(4) Engel, G. S.; Calhoun, T. R.; Read, E. L.; Ahn, T. K.; Mancal, T.; Cheng, Y. C.; Blankenship, R. E.; Fleming, G. R. *Nature* **2007**, *446*, 782.
(5) Lee, H.; Cheng, Y. C.; Fleming, G. R. *Science* **2007**, *316*, 1462.
(6) Mohseni, M.; Rebentrost, P.; Lloyd, S.; Aspuru-Guzik, A. *J. Chem. Phys.* **2008**, *129*, 9.
(7) Plenio, M. B.; Huelga, S. F. *New J. Phys.* **2008**, *10*, 113019.
(8) Rebentrost, P.; Mohseni, M.; Kassal, I.; Lloyd, S.; Aspuru-Guzik, A. *New J. Phys.* **2009**, *11*, 033003.
(9) Collini, E.; Scholes, G. D. *Science* **2009**, *323*, 369.
(10) Ishizaki, A.; Fleming, G. R. *Proc. Natl. Acad. Sci. U.S.A.* **2009**, *106*, 17255.
(11) Panitchayangkoon, G.; Hayes, D.; Fransted, K. A.; Caram, J. R.; Harel, E.; Wen, J. Z.; Blankenship, R. E.; Engel, G. S. *Proc. Natl. Acad. Sci. U.S.A.* **2010**, *107*, 12766.
(12) Mukamel, S. *Principles of Nonlinear Optical Spectroscopy*; Oxford University Press: New York, 1995.
(13) Ishizaki, A.; Fleming, G. R. *J. Phys. Chem. B* **2011**, *115*, 6227.
(14) Cho, M. H.; Yu, J. Y.; Joo, T. H.; Nagasawa, Y.; Passino, S. A.; Fleming, G. R. *J. Phys. Chem.* **1996**, *100*, 11944.
(15) Vaswani, H. M.; Stenger, J.; Fromme, P.; Fleming, G. R. *J. Phys. Chem. B* **2006**, *110*, 26303.
(16) Personov, R. I.; Alshitz, E. I.; Bykovska, La. *JETP Lett.* **1972**, *15*, 431.
(17) Rebane, L. A.; Gorokhovskii, A. A.; Kikas, J. V. *Appl. Phys. B: Photophys. Laser Chem.* **1982**, *29*, 235.
(18) Cho, M. H.; Fleming, G. R. *J. Chem. Phys.* **2005**, *123*, No. 114506.
(19) Jonas, D. M. *Annu. Rev. Phys. Chem.* **2003**, *54*, 425.
(20) Cho, M. H. *Chem. Rev.* **2008**, *108*, 1331.
(21) Yang, M. N.; Fleming, G. R. *J. Chem. Phys.* **1999**, *110*, 2983.
(22) Wendling, M.; Pullerits, T.; Przyjalgowski, M. A.; Vulto, S. I. E.; Aartsma, T. J.; van Grondelle, R.; van Amerongen, H. *J. Phys. Chem. B* **2000**, *104*, 5825.
(23) Cho, M. H.; Vaswani, H. M.; Brixner, T.; Stenger, J.; Fleming, G. R. *J. Phys. Chem. B* **2005**, *109*, 10542.
(24) Camara-Artigas, A.; Blankenship, R. E.; Allen, J. P. *Photosynth. Res.* **2003**, *75*, 49.
(25) Brixner, T.; Mancal, T.; Stiopkin, I. V.; Fleming, G. R. *J. Chem. Phys.* **2004**, *121*, 4221.
(26) Cowan, M. L.; Ogilvie, J. P.; Miller, R. J. D. *Chem. Phys. Lett.* **2004**, *386*, 184.
(27) Harel, E.; Fidler, A. F.; Engel, G. S. *J. Phys. Chem. A* **2011**, *115*, 3787.
(28) Harel, E.; Engel, G. S. Submitted for publication to *Proc. Natl. Acad. Sci. U.S.A.*, 2011.
(29) Fenna, R. E.; Matthews, B. W. *Nature* **1975**, *258*, 573.
(30) Mcdermott, G.; Prince, S. M.; Freer, A. A.; Hawthornthwaite-Lawless, A. M.; Papiz, M. Z.; Cogdell, R. J.; Isaacs, N. W. *Nature* **1995**, *374*, 517.
(31) Demirdoven, N.; Khalil, M.; Tokmakoff, A. *Phys. Rev. Lett.* **2002**, *89*, 4.
(32) van Veldhoven, E.; Khurmi, C.; Zhang, X. Z.; Berg, M. A. *ChemPhysChem* **2007**, *8*, 1761.